

See discussions, stats, and author profiles for this publication at: <https://www.researchgate.net/publication/244459814>

How do the electronic structures of low-symmetry metal-hydride and -alkyl complexes compare? Photoelectron spectroscopy and computational studies of $(\eta^5\text{-C}_5\text{R}_5)\text{Re}(\text{NO})(\text{L})\text{R}'(\text{L} = \text{CO}, \text{P}(\dots$

ARTICLE in ORGANOMETALLICS · DECEMBER 2002

Impact Factor: 4.13 · DOI: 10.1021/om020793t

CITATIONS

2

READS

87

8 AUTHORS, INCLUDING:



Nadine E Gruhn

University of Washington Seattle

79 PUBLICATIONS 2,597 CITATIONS

SEE PROFILE



Anjana Chaudhuri

shri agrasen girls college korba

12 PUBLICATIONS 219 CITATIONS

SEE PROFILE



John A Gladysz

Texas A&M University

251 PUBLICATIONS 7,065 CITATIONS

SEE PROFILE



Alain Igau

French National Centre for Scientific Research

111 PUBLICATIONS 1,173 CITATIONS

SEE PROFILE

How Do the Electronic Structures of Low-Symmetry Metal–Hydride and –Alkyl Complexes Compare? Photoelectron Spectroscopy and Computational Studies of $(\eta^5\text{-C}_5\text{R}_5)\text{Re}(\text{NO})(\text{L})\text{R}'$ ($\text{L} = \text{CO}, \text{P}(\text{C}_6\text{H}_5)_3$; $\text{R}, \text{R}' = \text{H}, \text{CH}_3$)

Dennis L. Lichtenberger,^{*,†,1} Nadine E. Gruhn,¹ Anjana Rai-Chaudhuri,¹ Sharon K. Renshaw,¹ John A. Gladysz,^{*,2,3} Haijun Jiao,³ Jeff Seyler,² and Alain Igau²

Center for Gas-Phase Electron Spectroscopy, Department of Chemistry, The University of Arizona, Tucson, Arizona 85721, Department of Chemistry, University of Utah, Salt Lake City, Utah 84112, and Institut für Organische Chemie, Friedrich-Alexander Universität Erlangen-Nürnberg, Henkestrasse 42, 91054 Erlangen, Germany

Received September 23, 2002

The electronic structures of $\text{CpRe}(\text{NO})(\text{L})\text{R}$ and $\text{Cp}^*\text{Re}(\text{NO})(\text{L})\text{R}$ ($\text{Cp} = \eta^5\text{-C}_5\text{H}_5$, $\text{Cp}^* = \eta^5\text{-C}_5(\text{CH}_3)_5$; $\text{L} = \text{CO}, \text{P}(\text{C}_6\text{H}_5)_3$; $\text{R} = \text{H}, \text{CH}_3$) are studied using gas-phase photoelectron spectroscopy and density functional theory. Separate valence ionizations from the three occupied metal-based orbitals of the d^6 Re center, the Re-R σ bond orbitals, and the predominantly $\text{Cp } e_1'' p_\pi$ orbitals are clearly observed. Comparison of the shapes and energies of the Cp and $\sigma(\text{Re-R})$ ionizations indicates an additional direct interaction between these orbitals that is sensitive to energy matching. This interaction results in a more delocalized σ -bonding framework for the methyl complexes than for the analogous hydrides and halides. The energy shifts and cross-sections of the metal-based ionizations provide quantitative measures of the different abilities of the nitrosyl, carbonyl, and phosphine ligands to delocalize and stabilize the metal electron density through π back-bonding. In these molecules the stabilization of a metal-based ionization by an NO ligand (~ 1.4 eV) is about twice that by a CO ligand (~ 0.7 eV), which is in turn about twice that by a $\text{P}(\text{C}_6\text{H}_5)_3$ ligand (~ 0.4 eV). The shifts of the metal-based ionization energies when the hydride ligand is replaced by methyl show that the methyl ligand is acting as a weak π donor. The first metal-based ionization shifts more than the second upon substitution of methyl for hydride, because it is less delocalized and consequently has more metal character for π interaction with the R ligand. This difference in the two metal π orbital distributions, along with the differences in energy, influences the rotational orientation of ligands at this site. The extent of this π interaction is sensitive to the electron richness at the metal center.

Introduction

Transition-metal hydride and alkyl complexes are ubiquitous intermediates in catalysis. Although their structures and bonding features are often quite similar, small differences clearly play pivotal roles in their respective chemistries. For example, hydride migrations to coordinated alkenes are orders of magnitude faster than the corresponding alkyl migrations.^{4,5} In contrast, carbonylations of metal hydrides to metal η^1 -formyls are nearly always endothermic, whereas carbonylations of metal alkyls to metal η^1 -acyls are often exothermic.^{6,7}

Much effort has been directed at the accurate description of the chemical, physical, and bonding properties of metal hydride and alkyl complexes.^{8–11} This continually expanding body of work includes values of bond dissociation energies from calorimetry,^{8,12–16} and gas-

* To whom correspondence should be addressed.

† E-mail: dlichten@u.arizona.edu.

(1) The University of Arizona.

(2) University of Utah.

(3) Friedrich-Alexander Universität Erlangen-Nürnberg.

(4) Brookhart, M.; Hauptman, E.; Lincoln, D. M. *J. Am. Chem. Soc.* **1992**, *114*, 10394–10401 and references therein.

(5) Rix, F. C.; Brookhart, M.; White, P. S. *J. Am. Chem. Soc.* **1996**, *118*, 2436–2448.

(6) Farnos, M. D.; Woods, B. A.; Wayland, B. B. *J. Am. Chem. Soc.* **1986**, *108*, 3659–3663 and references therein.

(7) Ellis, W. W.; Miedaner, A.; Curtis, C. J.; Gibson, D. H.; DuBois, D. L. *J. Am. Chem. Soc.* **2002**, *124*, 1926–1932.

(8) Nolan, S. P.; López De La Vega, R.; Mukerjee, S. L.; Gonzalez, A. A.; Zhang, K.; Hoff, C. D. *Polyhedron* **1988**, *7*, 1491–1498.

(9) Simões, J. A. M.; Beauchamp, J. L. *Chem. Rev.* **1990**, *90*, 629–688.

(10) *Bonding Energetics in Organometallic Compounds*; Marks, T. J., Ed.; ACS Symposium Series 428; American Chemical Society: Washington, DC, 1990.

(11) Klassen, J. K.; Selke, M.; Sorensen, A. A.; Yang, G. K. *J. Am. Chem. Soc.* **1990**, *112*, 1267–1268.

(12) Nolan, S. P.; López De La Vega, R.; Hoff, C. D. *J. Organomet. Chem.* **1986**, *315*, 187–199.

(13) Nolan, S. P.; López De La Vega, R.; Mukerjee, S. L.; Hoff, C. D. *Inorg. Chem.* **1986**, *25*, 1160–1165.

(14) Nolan, S. P.; Hoff, C. D.; Stoutland, P. O.; Newman, L. J.; Buchanan, J. M.; Bergman, R. G.; Yang, G. K.; Peters, K. S. *J. Am. Chem. Soc.* **1987**, *109*, 3143–3145.

(15) Calhorda, M. J.; Simoes, J. A. M. *Organometallics* **1987**, *6*, 1188–1190.

phase studies,^{17–23} measurements of metal hydride acidities,^{24–37} and the characterization of equilibria in Ziegler–Natta polymerization.^{38,39} Many theoretical studies have also been undertaken.^{15,22,23,40–50} We have sought to apply new experimental probes to these issues that are capable of delineating subtle electronic differences.

In this paper, we utilize gas-phase photoelectron spectroscopy to probe the electronic structures of a representative series of low-symmetry metal-hydride and -alkyl complexes of the general formulas $\text{CpRe}(\text{NO})(\text{CO})\text{R}$ and $\text{Cp}^*\text{Re}(\text{NO})(\text{CO})\text{R}$ ($\text{Cp} = \eta^5\text{-C}_5\text{H}_5$, $\text{Cp}^* = \eta^5\text{-C}_5(\text{CH}_3)_5$). Results from density functional theory calculations assist in illustrating the electronic structure features. In addition, the photoelectron spectra of the

phosphine analogues $\text{CpRe}(\text{NO})(\text{PPh}_3)\text{R}$ are obtained to study the electronic effect of phosphine substitution for CO, which gives insight into the electronic control of the stereoselective binding of organic ligands to the $[\text{CpRe}(\text{NO})(\text{PPh}_3)]^+$ fragment.⁵¹ These results also are compared to the spectra of $\text{CpRe}(\text{NO})(\text{CO})\text{X}$ ($\text{X} = \text{Cl}, \text{Br}, \text{I}$), which we have reported previously.⁵²

The valence spectra of these systems generally contain ionizations that are well-separated from each other in energy, which allows for the evaluation of subtle ionization energy shifts. The metal-based ionization energies of the formal d^6 metal centers of these molecules are all similarly sensitive to the inductive σ -electron donation of the ligands and electron richness at the metal center, while the splitting pattern of these ionizations is sensitive to the relative π -donation/acceptance properties of the ligands. Due to these advantages, the photoelectron spectra of these molecules clearly show a π -type interaction between occupied methyl ligand orbitals and metal fragment orbitals that has no counterpart for the hydride ligand. Previous theoretical calculations have suggested the presence of this filled–filled π interaction,^{41,42} but direct observation of the methyl π interaction separate from the σ -bonding effects is difficult to obtain by techniques other than photoelectron spectroscopy. Evidence for this type of interaction has been suggested in previous photoelectron studies of other metal-hydride and metal-alkyl molecules such as C_{4v} -symmetry $\text{M}(\text{CO})_5\text{R}$ and the isoelectronic system $\text{CpFe}(\text{CO})_2\text{R}$, but these studies had uncertainties due to close proximities of other ionizations or additional mixing of orbitals.^{53–56}

A methyl π interaction with the metal has implications for the different thermodynamic stability and reactivity trends often found for metal-alkyls as compared to metal-hydrides. When the metal d_π orbitals are occupied, this is a filled–filled π interaction with the methyl ligand that weakens the metal–methyl bond, but when the metal d_π orbitals are empty, the metal–methyl bond is strengthened. This point has been invoked to explain the trend that metal–methyl bonds are weaker than metal–hydride bonds for middle to late transition metals but are similar for early transition metals that lack electrons in the d_π orbitals. The π donor ability of the methyl ligand also allows evaluation of the relative importance of orbital energy and orbital overlap effects in controlling the preferred rotational orientation of unsymmetrical ligands bound to the metal center. For π acceptor ligands the orbital energy and orbital overlap effects act in the same direction, but for π donor ligands the effects are competing. The results reported here show the magnitude of the methyl π interaction in terms of its effects on the orbital energies and find it to be sensitive to the electron richness at the metal center by way of the competing

- (16) Wang, D.; Angelici, R. J. *J. Am. Chem. Soc.* **1996**, *118*, 935–942.
- (17) Stevens, A. E.; Beauchamp, J. L. *J. Am. Chem. Soc.* **1981**, *103*, 190–192.
- (18) Sallans, L.; Lane, K. R.; Squires, R. R.; Freiser, B. S. *J. Am. Chem. Soc.* **1985**, *107*, 4379–4385.
- (19) Armentrout, P. B.; Georgiadis, R. *Polyhedron* **1988**, *7*, 1573–1581.
- (20) Armentrout, P. B.; Kickel, B. L. In *Organometallic Ion Chemistry*; Freiser, B. S., Ed.; Kluwer: Dordrecht, The Netherlands, 1996; pp 1–45.
- (21) Freiser, B. S. *J. Mass. Spectrom.* **1996**, *31*, 703–715.
- (22) Chen, H.; Jacobsen, D. B.; Freiser, B. S. *Organometallics* **1999**, *18*, 5460–5469.
- (23) Zhang, X.-G.; Liyanage, R.; Armentrout, P. B. *J. Am. Chem. Soc.* **2001**, *123*, 5563–5575.
- (24) Pearson, R. G. *Chem. Rev.* **1985**, *85*, 41–49.
- (25) Moore, E. J.; Sullivan, J. M.; Norton, J. R. *J. Am. Chem. Soc.* **1986**, *108*, 2257–2263.
- (26) Crocco, G. L.; Gladysz, J. A. *J. Am. Chem. Soc.* **1988**, *110*, 6110–6118.
- (27) Edidin, R. T.; Sullivan, J. M.; Norton, J. R. *J. Am. Chem. Soc.* **1987**, *109*, 3945–3953.
- (28) Tilset, M.; Parker, V. D. *J. Am. Chem. Soc.* **1989**, *111*, 6711–6717.
- (29) Weberg, R. T.; Norton, J. R. *J. Am. Chem. Soc.* **1990**, *112*, 1105–1108.
- (30) Jia, G.; Morris, R. H. *J. Am. Chem. Soc.* **1991**, *113*, 875–883.
- (31) Miller, A. E. S.; Beauchamp, J. L. *J. Am. Chem. Soc.* **1991**, *113*, 8765–8770.
- (32) Jia, G.; Lough, A. J.; Morris, R. H. *Organometallics* **1992**, *11*, 161–171.
- (33) Kristjansd, O.; Norton, J. R. In *Transition Metal Hydrides*; Dedieu, A., Ed.; VCH: New York, 1992; Chapter 9.
- (34) Cappellani, E. P.; Drouin, S. D.; Jia, G.; Maltby, P. A.; Morris, R. H.; Schweitzer, C. T. *J. Am. Chem. Soc.* **1994**, *116*, 3375–3388.
- (35) Liu, W.; Thorp, H. H. *J. Am. Chem. Soc.* **1995**, *117*, 9822–9825.
- (36) Ng, W. S.; Jia, G.; Hung, M. Y.; Lau, C. P.; Wong, K. Y.; Wan, L. *Organometallics* **1998**, *17*, 4556–4561.
- (37) Abdur-Rashid, K.; Fong, T. P.; Greaves, B.; Gusev, D. G.; Hinman, J. G.; Landau, S. E.; Lough, A. J.; Morris, R. H. *J. Am. Chem. Soc.* **2000**, *122*, 9155–9171.
- (38) Tempel, D. J.; Johnson, L. K.; Huff, R. L.; White, P. S.; Brookhart, M. *J. Am. Chem. Soc.* **2000**, *122*, 6686–6700.
- (39) Shultz, L. H.; Tempel, D. J.; Brookhart, M. *J. Am. Chem. Soc.* **2001**, *123*, 11539–11555.
- (40) Schilling, J. B.; Goddard, W. A., III; Beauchamp, J. L. *J. Am. Chem. Soc.* **1987**, *109*, 5573–5580.
- (41) Ziegler, T.; Tschinke, V.; Becke, A. *J. Am. Chem. Soc.* **1987**, *109*, 1351–1358.
- (42) Ziegler, T.; Cheng, W.; Baerends, E. J.; Ravenek, W. *Inorg. Chem.* **1988**, *27*, 3458–3464.
- (43) Labinger, J. A.; Bercaw, J. E. *Organometallics* **1988**, *7*, 926–928.
- (44) Ziegler, T.; Tschinke, V. In *Bonding Energetics in Organometallic Compounds*; Marks, T. J., Ed.; ACS Symposium Series 428; American Chemical Society: Washington, DC, 1990; p 279.
- (45) Jackson, S. A.; Eisenstein, O.; Martin, J. D.; Albeniz, A. C.; Crabtree, R. H. *Organometallics* **1991**, *10*, 3062–3069.
- (46) Brougham, D. F.; Brown, D. A.; Fitzpatrick, N. J.; Glass, W. K. *Organometallics* **1995**, *14*, 151–156.
- (47) Ziegler, T. *Can. J. Chem.* **1995**, *73*, 743–761.
- (48) Antes, I.; Frenking, G. *Organometallics* **1995**, *14*, 4263–4268.
- (49) Han, Y.; Deng, L.; Ziegler, T. *J. Am. Chem. Soc.* **1997**, *119*, 5939–5945.
- (50) Papoian, G.; Nørskov, J. K.; Hoffmann, R. *J. Am. Chem. Soc.* **2000**, *122*, 4129–4144.

- (51) Gladysz, J. A.; Boone, B. J. *Angew. Chem., Int. Ed. Engl.* **1997**, *36*, 551–583.
- (52) Lichtenberger, D. L.; Rai-Chaudhuri, A.; Seidel, M. J.; Gladysz, J. A.; Agbossou, S. K.; Igau, A.; Winter, C. H. *Organometallics* **1991**, *10*, 1355–1364.
- (53) Lichtenberger, D. L.; Fenske, R. F. *Inorg. Chem.* **1974**, *13*, 486–488.
- (54) Hall, M. B. *J. Am. Chem. Soc.* **1975**, *97*, 2057–2065.
- (55) Lichtenberger, D. L.; Copenhaver, A. S. *J. Chem. Phys.* **1989**, *91*, 663–673.
- (56) Lichtenberger, D. L.; Gruhn, N. E.; Renshaw, S. K. *J. Mol. Struct.* **1997**, *405*, 79–86.

influences of the overlap and the energy match of the metal-based orbitals with the methyl orbitals.

Experimental Section

Preparation of Compounds. $\text{CpRe}(\text{NO})(\text{CO})\text{H}$,⁵⁷ $\text{CpRe}(\text{NO})(\text{CO})\text{CH}_3$,⁵⁸ $\text{Cp}^*\text{Re}(\text{NO})(\text{CO})\text{CH}_3$,⁵⁸ $\text{CpRe}(\text{NO})(\text{PPh}_3)\text{H}$,⁵⁹ and $\text{CpRe}(\text{NO})(\text{PPh}_3)\text{CH}_3$ ⁵⁹ were prepared according to literature procedures. Only partial preparative data have been reported for $\text{Cp}^*\text{Re}(\text{NO})(\text{CO})\text{H}$.^{58,60} Hence, full details of our synthesis and characterization follow.

A Schlenk flask was charged with $[\text{Cp}^*\text{Re}(\text{NO})(\text{CO})_2]^+\text{BF}_4^-$ (2.30 g, 4.65 mmol), acetone (25 mL), H_2O (3.0 mL, 167 mmol), $\text{N}(\text{CH}_2\text{CH}_3)_3$ (3.0 mL, 21.5 mmol), and a stir bar. The mixture was refluxed with stirring. After 10 h, solvent was removed by rotary evaporation. The oily residue was extracted with hexane (3×30 mL). Solvent was removed from the extracts, and the orange solid was dissolved in a minimum of CH_2Cl_2 . The solution was chromatographed on silica gel (28×2.5 cm column, 20:80 $\text{CH}_2\text{Cl}_2/\text{hexane}$ v/v). Solvent was removed from the orange band to give $\text{Cp}^*\text{Re}(\text{NO})(\text{CO})\text{H}$, which was dried under oil pump vacuum (1.33 g, 3.49 mmol, 75%); mp 91°C dec. Anal. Calcd for $\text{C}_{11}\text{H}_{16}\text{NO}_2\text{Re}$: C, 34.73; H, 4.24. Found: C, 34.80; H, 4.23. IR (cm^{-1} , KBr): 1994 m, 1947 vs, 1928 vs, 1689 vs, 1660 vs. ^1H NMR (δ , CD_2Cl_2): 2.01 (s, 5 CH_3), -7.79 (s, ReH). $^{13}\text{C}\{^1\text{H}\}$ NMR (ppm, CD_2Cl_2): 214.58 (s, CO), 102.04 (s, CCH_3), 11.18 (s, CH_3). MS (EI, m/z , ^{187}Re , 17 eV): 381 (M^+ , 89%), 351 ($\text{M}^+ - \text{NO}$, 100%).

Data Collection. Photoelectron spectra were recorded using an instrument that features a 36 cm hemispherical analyzer (McPherson) and custom-designed sample cells and detection and control electronics. The instrument and data collection and manipulation procedures have been described in detail elsewhere.⁵² During data collection the instrument resolution (measured using the full width at half-maximum of the argon $2\text{P}_{3/2}$ peak) was 0.016–0.022 eV. All samples sublimed cleanly with no detectable evidence of decomposition products in the gas phase or as a solid residue. The sublimation temperatures ($\pm 5^\circ\text{C}$, at 10^{-4} Torr) were as follows: $\text{CpRe}(\text{NO})(\text{CO})\text{H}$, 40°C ; $\text{CpRe}(\text{NO})(\text{CO})\text{CH}_3$, 55°C ; $\text{Cp}^*\text{Re}(\text{NO})(\text{CO})\text{H}$, 55°C ; $\text{Cp}^*\text{Re}(\text{NO})(\text{CO})\text{CH}_3$, 70°C ; $\text{CpRe}(\text{NO})(\text{PPh}_3)\text{H}$, 170°C ; $\text{CpRe}(\text{NO})(\text{PPh}_3)\text{CH}_3$, 170°C (monitored using a “K” type thermocouple passed through a vacuum feed-through and attached directly to the sample cell). Valence region spectra of all the compounds investigated are shown in Figure 1.

The spectra are represented analytically with the best fit of asymmetric Gaussians. Each Gaussian is defined with the position, amplitude, half-width for the high binding energy side, and half-width for the low binding energy side. The peak positions and half-widths are reproducible to about ± 0.02 eV ($\sim 3\sigma$ level). The number of peaks used in a spectral deconvolution was based solely on the features of a given band profile. The parameters describing an individual ionization peak are less certain when two or more peaks are close in energy and overlap. The deconvolution procedures are described in more detail elsewhere.⁶¹

Computational Methodology. Density functional computations were carried out using the Gaussian 98 program.⁶² Geometries were fully optimized at the B3LYP hybrid density functional level of theory using the LANL2DZ basis set augmented with an additional set of polarization functions

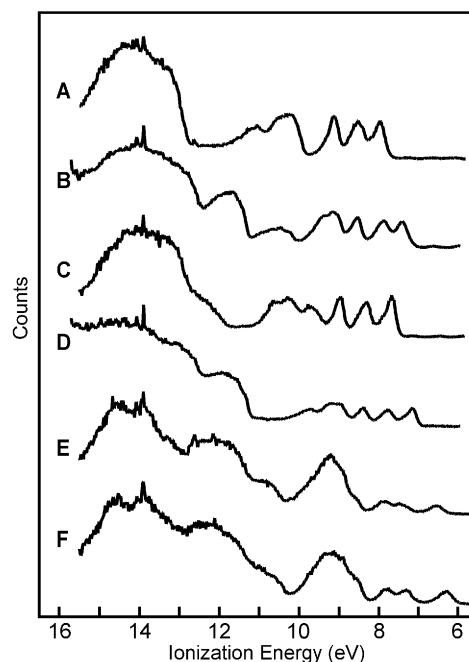


Figure 1. Valence photoelectron spectra of (A) $\text{CpRe}(\text{NO})(\text{CO})\text{H}$, (B) $\text{CpRe}(\text{NO})(\text{CO})\text{CH}_3$, (C) $\text{Cp}^*\text{Re}(\text{NO})(\text{CO})\text{H}$, (D) $\text{Cp}^*\text{Re}(\text{NO})(\text{CO})\text{CH}_3$, (E) $\text{CpRe}(\text{NO})(\text{PPh}_3)\text{H}$, and (F) $\text{CpRe}(\text{NO})(\text{PPh}_3)\text{CH}_3$.

(LANL2DZp).^{63,64} Frequency calculations at the same level indicate that all optimized geometries are true minima on the potential energy surface.⁶⁵ Orbital plots were generated using the program Molekel.⁶⁶ The first vertical ionization energy (IE_1) is defined as the difference between the single-point energy (E^+) of the radical cation frozen at the neutral geometry and the energy (E^0) of the fully optimized neutral molecule. The higher energy ion states would not converge in this manner, due to the low symmetry of the molecules; therefore, the ionization energy corresponding to removal of an electron from occupied orbital n is defined as $\text{IE}_n = \text{IE}_1 + (\epsilon_{\text{HOMO}} - \epsilon_n)$, where ϵ_{HOMO} and ϵ_n are the eigenvalues of the designated orbitals for the neutral molecule. The calculated total electronic energies and coordinates for the optimized geometries are summarized in the Supporting Information.

Preliminary Theoretical Considerations

Before introducing the photoelectron data, it is helpful to consider the qualitative electronic structure of $\text{CpRe}(\text{NO})(\text{L})\text{R}$ molecules⁶⁷ with particular attention to the

(57) Sweet, J. R.; Graham, W. A. G. *Organometallics* **1982**, *1*, 982–986.

(58) Sweet, J. R.; Graham, W. A. G. *J. Am. Chem. Soc.* **1982**, *104*, 2811–2815.

(59) Agbossou, F.; O'Connor, E. J.; Garner, C. M.; Quirós Méndez, N.; Fernández, J. M.; Patton, A. T.; Ramsden, J. A.; Gladysz, J. A. *Inorg. Synth.* **1992**, *29*, 211–225.

(60) Chinn, M. S.; Heinekey, D. M.; Payne, N. G.; Sofield, C. D. *Organometallics* **1989**, *8*, 1824–1826.

(61) Lichtenberger, D. L.; Copenhaver, A. S. *J. Electron Spectrosc. Relat. Phenom.* **1990**, *50*, 335–352.

(62) Frisch, M. J.; Trucks, G. W.; Schlegel, H. B.; Scuseria, G. E.; Robb, M. A.; Cheeseman, J. R.; Zakrzewski, V. G.; Montgomery, J. J. A.; Stratmann, R. E.; Burant, J. C.; Dapprich, S.; Millam, J. M.; Daniels, A. D.; Kudin, K. N.; Strain, M. C.; Farkas, O.; Tomasi, J.; Barone, V.; Cossi, M.; Cammi, R.; Mennucci, B.; Pomelli, C.; Adamo, C.; Clifford, S.; Ochterski, J.; Peterson, G. A.; Ayala, P. Y.; Cui, Q.; Morokuma, K.; Malick, D. K.; Rabuck, A. D.; Raghavachari, K.; Foresman, J. B.; Cioslowski, J.; Ortiz, J. V.; Stefanov, B. B.; Liu, G.; Liashenko, A.; Piskorz, P.; Komaromi, I.; Gomperts, R.; Martin, R. L.; Fox, D. J.; Keith, T.; Al-Laham, M. A.; Peng, C. Y.; Nanayakkara, A.; Gonzalez, C.; Challacombe, M.; Gill, P. M. W.; Johnson, B.; Chen, W.; Wong, M. W.; Andres, J. L.; Head-Gordon, M.; Replogle, E. S.; Pople, J. A. *Gaussian 98*; Gaussian, Inc.: Pittsburgh, PA, 1998.

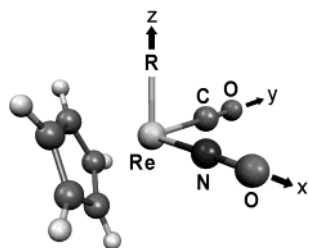
(63) Hay, P. J.; Wadt, W. R. *J. Chem. Phys.* **1985**, *82*, 299–310.

(64) Huzinaga, S.; Anzelm, J.; Klobukowski, M.; Radzio-Andzelm, E.; Sakai, Y.; Tatewaki, H. *Gaussian Basis Sets for Molecular Calculations*; Elsevier: Amsterdam, 1984.

(65) Foresman, J. B.; Frisch, A. *Exploring Chemistry with Electronic Structure Methods: A Guide to Using Gaussian*, 2nd ed.; Gaussian, Inc.: Pittsburgh, PA, 1996.

(66) Flukiger, P.; Luthi, H. P.; Portmann, S.; Weber, J. *Molekel 4.1*; Swiss Center for Scientific Computing: Manno, Switzerland, 2000–2001.

features that are important to the information provided by these experiments. In a first-order analysis the changes in ionization energies observed as chemical substitutions are made throughout the molecule are interpreted in terms of changes in the orbital energies in the ground state of the molecules. All of the ionizations observed will be influenced by changes in the net charge potential felt throughout the molecule due to the inductive influences caused by ligand substitutions. In addition, the metal-based ionizations of these molecules will be influenced by metal-ligand π -orbital overlap interactions. While $\text{CpRe}(\text{NO})(\text{CO})\text{R}$ molecules strictly have no symmetry, there is considerable symmetry separation of the σ and π interactions between the metal and ligands due to the strong π interactions of NO and CO and the near 90° angles between ligands. In a coordinate system such as that shown below with the NO ligand on the x axis, the CO ligand on the y axis, and the hydride or methyl ligand on the z axis, the d^6 metal levels of t_{2g} heritage (from O_h symmetry) of the $[\text{CpRe}(\text{NO})(\text{CO})]^+$ fragment are predominantly the d_{xz} , d_{yz} , and d_{xy} orbitals.



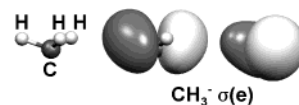
The d_{xy} orbital back-bonds extensively into the NO and CO π^* orbitals, which makes the d_{xy} -based orbital the most stable of the three filled metal-based orbitals. This orbital has predominantly δ symmetry with respect to the open coordination site and, therefore, has essentially no π -bonding capability with R. The d_{yz} orbital back-bonds into the CO π^* orbital and can also interact with orbitals on R that have π symmetry with respect to the metal-R bond. The d_{xz} orbital has the correct symmetry to back-bond into the NO π^* orbital and also to interact with orbitals on R that have π symmetry along the metal-R bond. The different π -back-bonding capabilities of the ligands cause these three filled metal-based orbitals to be well separated in energy. Previous photoelectron studies on d^6 molecules of general formula $\text{CpM}(\text{CO})_2\text{L}$ have shown that π back-bonding to a nitrosyl ligand stabilizes a metal-based ionization by about 1.5 eV, whereas π back-bonding to a carbonyl ligand stabilizes a metal-based ionization by about 0.7 eV.⁵⁶ Using these observations, the d_{yz} -based ionization would be stabilized about 0.7 eV by the carbonyl, the d_{xz} -based ionization would be stabilized by about 1.5 eV by the nitrosyl, and the d_{xy} -based ionization would be stabilized by about 2.2 eV by the combination of the nitrosyl and the carbonyl π back-bonding. The differences in these stabilizations predict about 0.7 eV separations between each of the metal-based ionizations. This is in contrast to the isoelectronic $[\text{CpFe}(\text{CO})_2]^+$ fragment,⁶⁸ for which the d_{xz} and d_{yz} orbitals combine in back-bonding to the carbonyls and there is

only a small energy splitting between the resulting two orbitals from lack of true C_{4v} symmetry. As will be shown, the photoelectron spectra reported here serve as test cases to see if these expected splitting values are transferable.

Three other orbitals of the $[\text{CpRe}(\text{NO})(\text{CO})]^+$ fragment that must be considered in the low-energy region of ionizations are the two e_1'' -based orbitals from the Cp ring π system and the LUMO. In higher symmetry molecules such as $\text{CpMn}(\text{CO})_3$, the two Cp orbitals transform as an e set, but in the lower symmetry of the $[\text{CpRe}(\text{NO})(\text{CO})]^+$ fragment this strict degeneracy is lost. One of the predominantly Cp orbitals has some $d_{x^2-y^2}$ character, while the other Cp orbital has some d_{z^2} character. The LUMO of the $[\text{CpRe}(\text{NO})(\text{CO})]^+$ fragment derives from one of the orbitals of the metal d_{eg} level (in O_h symmetry), which are the antibonding counterparts of the metal-ligand σ bonds. The LUMO is predominantly metal d_{z^2} but also contains some Cp ring π character.

Three-dimensional representations of the six resultant valence molecular orbitals of $\text{CpRe}(\text{NO})(\text{CO})\text{H}$ as calculated by density functional theory (vide infra) are shown in Figure 2. The three predominantly metal d orbitals are labeled $M1_{\text{CO,R}}$, $M2_{\text{NO,R}}$, and $M3_{\text{NO,CO}}$ in Figure 2 to emphasize the ligands with which each orbital interacts in a π fashion. Interaction between the $[\text{CpRe}(\text{NO})(\text{CO})]^+$ fragment and a H^- ligand primarily involves donation from the occupied 1s orbital of the hydride ligand into the empty LUMO of the $[\text{CpRe}(\text{NO})(\text{CO})]^+$ fragment to form the $\sigma(\text{Re}-\text{H})$ bond.

Like the hydride ligand, interaction of the $[\text{CpRe}(\text{NO})(\text{CO})]^+$ fragment with a CH_3^- ligand also involves donation from a σ -donor orbital, in this case the CH_3^- sp^3 orbital, into the $[\text{CpRe}(\text{NO})(\text{CO})]^+$ fragment LUMO. As will be shown, mixing between Cp and $\sigma(\text{Re}-\text{C})$ orbitals occurs, and the resultant σ delocalization is much more extensive for the methyl molecules than for the hydrides.⁶⁹ Unlike the hydride ligand, the methyl ligand also has an occupied e set of C-H bonding orbitals,⁷⁰⁻⁷² shown in the orbital surface plots:⁷³



These orbitals have the possibility of an additional π interaction with the metal that is not possible with a hydride ligand. The photoelectron ionizations allow measurement of the magnitude of this interaction.

Results

Photoelectron Spectra. For each of the spectra reported here the region from approximately 6 to 12 eV

(68) Schilling, B. E. R.; Hoffman, R.; Lichtenberger, D. L. *J. Am. Chem. Soc.* **1979**, *101*, 585-591.

(69) Lichtenberger, D. L.; Gruhn, N. E.; Rai-Chaudhuri, A.; Renshaw, S. K.; Gladysz, J. A.; Jiao, H.; Seyler, J.; Igau, A. *J. Am. Chem. Soc.* **2002**, *124*, 1417-1423.

(70) Libit, L.; Hoffmann, R. *J. Am. Chem. Soc.* **1974**, *96*, 1370-1383.

(71) DeFrees, D. J.; Bartmess, J. F.; Kim, J. K.; McIver, R. T., Jr.; Hehre, W. H. *J. Am. Chem. Soc.* **1977**, *99*, 6451-6452.

(72) Apeloig, Y.; Schleyer, P. v. R.; Pople, J. A. *J. Am. Chem. Soc.* **1977**, *99*, 5901-5909.

(73) Orbitals obtained from a Hartree-Fock calculation using the basis set described in the Experimental Section and displayed at the 0.05 surface value.

(67) Schilling, B. E. R.; Hoffmann, R.; Faller, J. *J. Am. Chem. Soc.* **1979**, *101*, 592-598.

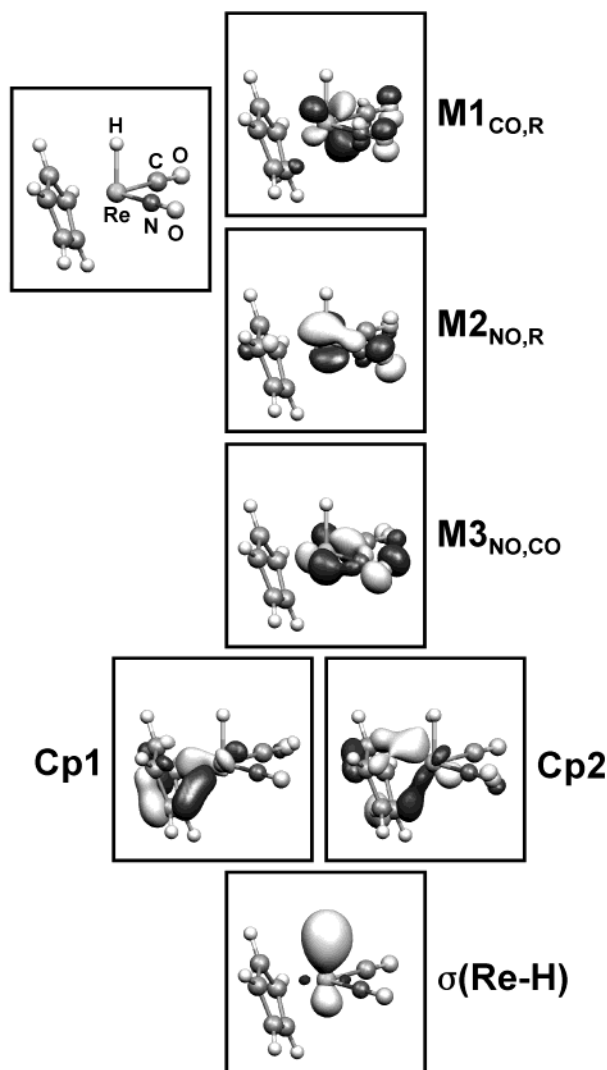


Figure 2. Orbital contour plots (value ± 0.08) of valence orbitals of $\text{CpRe}(\text{NO})(\text{CO})\text{H}$. Atomic positions are labeled in the ball-and-stick drawing in the upper left-hand corner.

contains the ionization bands corresponding to removal of an electron from each of the orbitals described in the previous section. The He I and He II spectra for $\text{CpRe}(\text{NO})(\text{CO})\text{H}$, $\text{CpRe}(\text{NO})(\text{CO})\text{CH}_3$, $\text{Cp}^*\text{Re}(\text{NO})(\text{CO})\text{H}$, and $\text{Cp}^*\text{Re}(\text{NO})(\text{CO})\text{CH}_3$ in this region are shown in Figure 3. Information from the analytical representations of the numerical data in terms of asymmetric Gaussians is given in Table 1. The primary character associated with an ionization is assigned by comparing He I and He II photoelectron spectra and by comparing changes within the series. The labels of ionizations listed in Table 1 reflect the primary character of the valence metal or ligand orbitals. However, it must be remembered that a completely accurate description of an orbital from which an ionization originates most often includes character from other valence metal or ligand orbitals. This mixing is critically important for understanding the electronic structure and behavior of these molecules and will be considered in greater detail in the Discussion.

The spectra of $\text{CpRe}(\text{NO})(\text{PPh}_3)\text{H}$ and $\text{CpRe}(\text{NO})(\text{PPh}_3)\text{CH}_3$ are complicated by the presence of phenyl ring π ionizations near 9 eV, which obscure all but the metal-based ionizations. These metal-based ionizations

Table 1. Fit Parameters^a and Assignments of Ionizations

| position | half-width high, low | rel area ^b | | label | calcd vertical ionization energy ^c |
|--|-------------------------|-----------------------|------------|-----------------------|---|
| | | He I | He II/He I | | |
| CpRe(NO)(CO)H | | | | | |
| 7.96 | 0.41, 0.28 | 1.11 | 0.76 | M1 | 8.10 (6.16) |
| 8.50 | 0.55, 0.35 | 1.26 | 0.90 | M2 | 8.54 |
| 9.09 | 0.47, 0.20 | 1 | 1 | M3 | 9.18 |
| 10.14 | 0.51, 0.36 | 1.14 | 0.63 | Cp1 | 10.15 |
| 10.55 | 0.51, 0.36 | 0.83 | 0.64 | Cp2 | 10.38 |
| 11.03 | | | | $\sigma(\text{Re-H})$ | 11.07 |
| CpRe(NO)(CO)CH ₃ | | | | | |
| 7.65 | 0.53, 0.18 | 1.22 | 0.75 | M1 | 7.76 (5.95) |
| 8.32 | 0.51, 0.27 | 1.15 | 0.95 | M2 | 8.19 |
| 8.97 | 0.37, 0.22 | 1 | 1 | M3 | 8.92 |
| 9.69 | 0.72, 0.58 | 1.56 | 0.56 | $\sigma(\text{Re-C})$ | 9.55 |
| 10.27 | 0.58, 0.38 | 1.40 | 0.64 | Cp1 | 10.00 |
| 10.64 | 0.63, 0.27 | 0.79 | 0.57 | Cp2 | 10.3 |
| Cp*Re(NO)(CO)H | | | | | |
| 7.43 | 0.39, 0.33 | 1.05 | 0.84 | M1 | 7.42 (5.69) |
| 7.87 | 0.54, 0.30 | 1.20 | 0.91 | M2 | 7.84 |
| 8.54 | 0.40, 0.24 | | 1 | M3 | 8.55 |
| 9.09 | 0.60, 0.33 | 1.71 | 0.73 | Cp1 | 8.96 |
| 9.46 | 0.56, 0.29 | 0.79 | 0.59 | Cp2 | 9.25 |
| 10.46 | | | | $\sigma(\text{Re-H})$ | 10.42 |
| Cp*Re(NO)(CO)CH ₃ | | | | | |
| 7.14 | 0.49, 0.18 | 1.06 | 0.81 | M1 | 7.17 (5.52) |
| 7.76 | 0.49, 0.2 | 1.08 | 1.06 | M2 | 7.54 |
| 8.39 | 0.43, 0.25 | 1 | 1 | M3 | 8.31 |
| 8.98 | 0.68, 0.34 | 1.87 | 0.77 | Cp2 | 8.78 |
| 9.33 | 0.68, 0.3 | 0.75 | 0.67 | Cp1 | 8.98 |
| 9.76 | 0.83, 0.29 | 1.04 | 0.5 | $\sigma(\text{Re-C})$ | 9.49 |
| CpRe(NO)(PPh ₃)H | | | | | |
| 6.53 | 0.58, 0.33 | 1 | | M1 | 6.59 ^d (4.94) ^d |
| 7.45 | 0.55, 0.41 | 1.02 | | M2 | 7.15 ^d |
| 7.87 | 0.53, 0.28 | 1.10 | | M3 | 7.76 ^d |
| CpRe(NO)(PPh ₃)CH ₃ | | | | | |
| 6.31 | 0.53, 0.34 | 1 | | M1 | 6.27 ^e (4.71) ^e |
| 7.35 | 0.52, 0.37 | 0.99 | | M2 | 6.98 ^e |
| 7.83 | 0.45, 0.30 | 0.85 | | M3 | 7.58 ^e |

^a All energies in eV. ^b Relative to peak assigned area = 1. ^c The number in parentheses is the absolute value of the HOMO orbital energy. The first ionization energy is defined as the difference between the single-point energy of the radical cation frozen at the neutral geometry and the energy of the fully optimized neutral molecule. Higher ionization energies are defined as the absolute orbital energies shifted by the difference between the HOMO orbital energy and the first ionization energy. ^d $\text{CpRe}(\text{NO})(\text{PMe}_3)\text{H}$. ^e $\text{CpRe}(\text{NO})(\text{PMe}_3)\text{CH}_3$; geometry taken from ref 88.

are shown in Figure 4 with the parameters of analytical representations again listed in Table 1.

The relative intensities of the ionization bands in spectra obtained with a He II source differ from those in spectra obtained with a He I source because of the different source-energy dependence of photoionization cross-sections for different orbitals. For He II spectra, Table 1 lists only the relative changes in areas from He I to He II excitation. From calculations, the photoionization cross-sections for rhenium 5d, oxygen 2p, nitrogen 2p, carbon 2p, and hydrogen 1s orbitals decrease by factors of 2.3, 1.6, 2.2, 3.2, and 6.6, respectively, in He II mode as compared to He I.⁷⁴ Assuming that molecular ionization cross-sections are a sum of atomic contributions (the Gelius model),⁷⁵ the change in the area of an ionization can give an indication of the origin

(74) Yeh, J.; Lindau, I. *At. Data Nucl. Data Tables* **1985**, 32, 1–155.

(75) Gelius, U. *J. Electron Spectrosc. Relat. Phenom.* **1974**, 5, 985–1057.

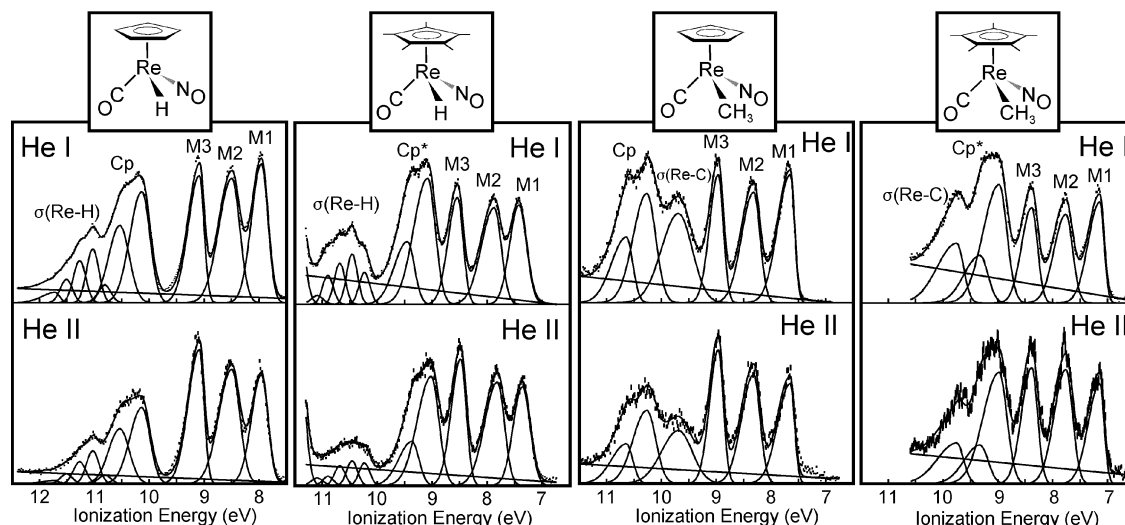


Figure 3. He I and He II photoelectron spectra of $\text{CpRe}(\text{NO})(\text{CO})\text{H}$, $\text{Cp}^*\text{Re}(\text{NO})(\text{CO})\text{H}$, $\text{CpRe}(\text{NO})(\text{CO})\text{CH}_3$, and $\text{Cp}^*\text{Re}(\text{NO})(\text{CO})\text{CH}_3$.

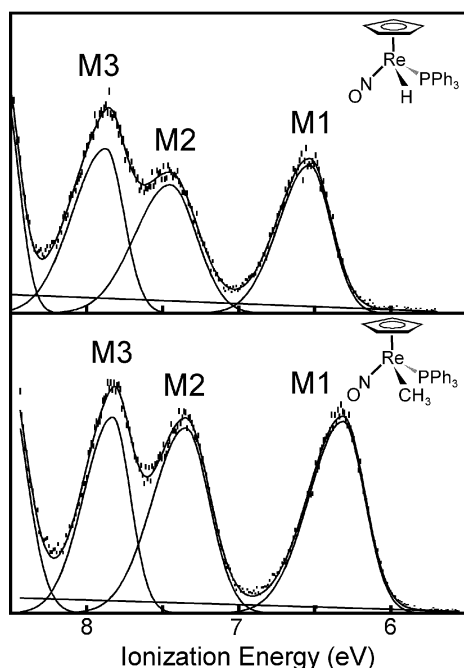


Figure 4. He I photoelectron spectra of the metal ionizations of $\text{CpRe}(\text{NO})(\text{PPh}_3)\text{H}$ and $\text{CpRe}(\text{NO})(\text{PPh}_3)\text{CH}_3$.

of the ionization band. Those bands that originate from orbitals with more rhenium, oxygen, and nitrogen character increase in area with He II excitation relative to ionizations that originate from orbitals with more carbon or hydrogen character.

$\text{CpRe}(\text{NO})(\text{CO})\text{H}$ and $\text{Cp}^*\text{Re}(\text{NO})(\text{CO})\text{H}$. The spectrum of $\text{CpRe}(\text{NO})(\text{CO})\text{H}$ has three ionization bands from 7.5 to 9.5 eV that originate from the predominantly Re d orbitals. As previously mentioned, the spacings of these ionizations reflect the different π -bonding interactions of the Re d orbitals with NO, CO, and H ligands. The ionization near 10.4 eV has the characteristic shape of a Cp ring ionization^{76,77} and is best modeled with two Gaussians. The remaining ionization envelope from 11

to 12 eV is assigned to ionization from the Re–H σ bond orbital. Although this ionization partially overlaps with the Cp ionization, it is still possible to see the unusual contour and shape. There are noticeable shoulders on the ionization, and it is not modeled well with a single Gaussian peak. These shoulders on the ionization are partially resolved vibrational energy levels in the positive ion. This vibrational information provides a measure of the change in force constant and equilibrium bond distance when an electron is removed from the σ -(Re–H) orbital. A detailed analysis of this structure is reported elsewhere.⁶⁹

Like the Cp analogue, the three relatively sharp ionization bands from about 7 to 8.5 eV in the spectra of $\text{Cp}^*\text{Re}(\text{CO})(\text{CO})\text{H}$ are the three ionizations from predominantly Re d orbitals. The bands at 9.09 and 9.46 eV have the characteristic shape and splitting of Cp^* ring ionizations in three-legged piano-stool molecules. The remaining ionization envelope from 10.0 to 11.3 eV is assigned to ionization from the σ (Re–H) bond orbital. The methylation of the Cp ligand causes the Cp^* ionization of $\text{Cp}^*\text{Re}(\text{CO})(\text{CO})\text{H}$ to be destabilized by about 1.1 eV from the Cp ionization of $\text{CpRe}(\text{CO})(\text{CO})\text{H}$, but the σ (Re–H) vertical ionization is only destabilized 0.57 eV. Because of the difference in these ionization shifts, the σ (Re–H) ionization of $\text{Cp}^*\text{Re}(\text{CO})(\text{CO})\text{H}$ is well separated from the Cp^* ionization and the vibrational structure in σ (Re–H) is more clearly observed.

The He II spectra of $\text{CpRe}(\text{NO})(\text{CO})\text{H}$ and $\text{Cp}^*\text{Re}(\text{NO})(\text{CO})\text{H}$ help to confirm the assignments. The Cp ionizations decrease by about 40% relative to the M3 ionization, which is similar to the behavior observed for the Cp ionizations of other piano-stool molecules. The σ (Re–H) ionizations decrease by 50% for $\text{CpRe}(\text{NO})(\text{CO})\text{H}$ and 55% for $\text{Cp}^*\text{Re}(\text{NO})(\text{CO})\text{H}$, which indicates significant hydrogen character in the corresponding Re–H σ bond orbitals.

$\text{CpRe}(\text{NO})(\text{CO})\text{CH}_3$ and $\text{Cp}^*\text{Re}(\text{NO})(\text{CO})\text{CH}_3$. The spectrum of $\text{CpRe}(\text{NO})(\text{CO})\text{CH}_3$ also contains three distinct ionizations from 7.5 to 9.5 eV that originate from predominantly metal-based orbitals. The remaining ionization envelope from 9.5 to 11 eV contains the Cp ring π and rhenium–carbon σ bond ionizations and is best modeled with three Gaussian peaks. In the He

(76) Calabro, D. C.; Hubbard, J. L.; Blevins, C. H., II; Campbell, A. C.; Lichtenberger, D. L. *J. Am. Chem. Soc.* **1981**, *103*, 6839–6846.

(77) Lichtenberger, D. L.; Fan, H.-J.; Gruhn, N. E.; Bitterwolf, T. E.; Gallagher, S. *Organometallics* **2000**, *19*, 2012–2021.

II spectrum, the areas of these three peaks all decrease by approximately the same amount, which suggests that they have similar amounts of rhenium and carbon character. The ionizations at 10.27 and 10.64 eV have the characteristic splitting, but unusual shape, for Cp ionizations. These features suggest unusual mixing as compared to that in other piano-stool molecules. The ionization assigned predominantly to $\sigma(\text{M}-\text{C})$ does not show the vibrational fine structure that the $\sigma(\text{M}-\text{H})$ ionization does, most likely because the frequency of a Re–C stretching vibration (~ 0.06 eV) approaches the limit of resolution for the experiment and perhaps also because of the greater mixing of this state indicated by the unusual ionization energy shifts. This mixing will be described more completely in the Discussion.

The spectrum of $\text{Cp}^*\text{Re}(\text{NO})(\text{CO})\text{CH}_3$ shows that the shape of the bands at 9 eV is characteristic for a Cp^* ring π ionization and is labeled as such. The band at 9.76 eV is assigned to the ionization from the $\sigma(\text{M}-\text{C})$ σ bond orbital. Note for later discussion that for $\text{Cp}^*\text{Re}(\text{NO})(\text{CO})\text{CH}_3$ the predominantly $\sigma(\text{M}-\text{C})$ ionization is assigned at higher ionization energy than the Cp^* ionizations, whereas in the previous case of $\text{CpRe}(\text{NO})(\text{CO})\text{CH}_3$ the predominantly $\sigma(\text{M}-\text{C})$ ionization is assigned at lower ionization energy than the Cp ionizations.

$\text{CpRe}(\text{NO})(\text{PPh}_3)\text{H}$ and $\text{CpRe}(\text{NO})(\text{PPh}_3)\text{CH}_3$. For these molecules only the metal-based ionizations can be observed clearly. Substitution of a CO ligand with a PPh_3 ligand results in general destabilization of the M1, M2, and M3 ionization bands by over 1 eV. M1 and M3 shift the most, consistent with the reduction in π -acceptor stabilization of these orbitals when CO is replaced by PPh_3 . Further, M3 shifts less than M1, consistent with the additional delocalization of this orbital to the NO ligand. The significance of these shifts to measurement of the π -acceptor ability of PPh_3 and to the electronic control of the orientation of single-faced π -acceptor ligands will be presented in the Discussion.

Computational Results. To see how theoretical treatment of these molecules compares to experiment, density functional computations were performed. Calculated vertical ionization energies are listed in Table 1, and orbital surface plots for the six highest occupied molecular orbitals of $\text{CpRe}(\text{NO})(\text{CO})\text{H}$ are shown in Figure 2. Further details are available in the Supporting Information. There is both qualitative (orbital character) and quantitative (ionization energies) agreement between theory and experiment. The orbital ordering calculated for each molecule agrees with the ordering of the six ionizations of interest, as indicated by experiment. Specifically, the first three occupied orbitals are calculated to have large rhenium d character and CO and NO ligand contributions, as anticipated in the preliminary considerations. For $\text{CpRe}(\text{NO})(\text{CO})\text{H}$, HOMO-3 and HOMO-4 are primarily Cp ligand in character with some metal d character, and HOMO-5 is the localized Re–H σ orbital with an orbital character of 45% for hydrogen and 51% for rhenium. The order of these three orbitals changes for $\text{CpRe}(\text{NO})(\text{CO})\text{CH}_3$ in agreement with the experimental assignment, with the Re–CH₃ σ orbital as HOMO-3 (56% carbon and 41% rhenium). The orbital HOMO-5 has contributions from

Cp, metal d orbital, and most importantly from CH₃, which will be explained further in the Discussion.

Discussion

Analysis of the ionization shifts caused by chemical substitutions gives insight into the nature of the filled metal orbitals and the extent of ligand σ and π mixing throughout the molecular framework. These shifts will be discussed in the following sections in terms of the effects of permethylation of the ring, the effects of substitution of methyl for hydride at the metal, and the effects of substitution of phosphine for CO at the metal. Comparison also is made to previously reported data on $\text{CpRe}(\text{NO})(\text{CO})\text{X}$ ($\text{X} = \text{Cl}, \text{Br}, \text{I}$).⁵² We will begin with discussion of the results that give information on the σ -bonding framework and follow with discussion of the metal-based ionizations, which give information on π interactions with the ligands. Last, the insight that these experimental results give into the electronic control of the stereoselective binding of organic ligands to the $[\text{CpRe}(\text{NO})(\text{L})]^+$ fragment will be described.

Re–H Bond. The vibrational structure observed on the $\sigma(\text{Re}-\text{H})$ ionizations of $\text{CpRe}(\text{NO})(\text{CO})\text{H}$ and $\text{Cp}^*\text{Re}(\text{NO})(\text{CO})\text{H}$ clearly identifies this ionization and can be used to directly determine the vibrational and equilibrium bond length changes that occur when an electron is removed from the $\sigma(\text{Re}-\text{H})$ orbital. A detailed study of the $\sigma(\text{Re}-\text{H})$ ionization vibrational structure as well as that for the $\sigma(\text{Re}-\text{D})$ ionization of $\text{Cp}^*\text{Re}(\text{NO})(\text{CO})\text{D}$ has been described elsewhere.⁶⁹ Franck–Condon simulations of the vibrational profiles show that the Re–H bond distances lengthen upon removal of an electron by 0.25(1) Å. This large bond distance change corresponds to a substantial weakening of the Re–H bond upon removal of an electron. This result, as well as observation of the deuterium isotope effect on the vibrational structure of the photoelectron ionization, has shown the Re–H bonding orbital to be highly localized.

Effects of Permethylation. In piano-stool molecules, permethylation of the Cp ring has fairly predictable effects on the energies of ionization bands and can give supporting evidence for the origin of an ionization. Permethylation typically destabilizes metal-based ionizations by ~ 0.6 eV, and ring- π -based ionizations by ~ 1.1 eV.⁷⁶ These trends are generally followed in the spectra of the metal–hydride molecules, where the metal bands shift to lower ionization energy by an average of 0.57 eV on going from $\text{CpRe}(\text{NO})(\text{CO})\text{H}$ to $\text{Cp}^*\text{Re}(\text{NO})(\text{CO})\text{H}$. The ring π -based ionizations are destabilized by an average of 1.07 eV in $\text{Cp}^*\text{Re}(\text{NO})(\text{CO})\text{H}$. The $\sigma(\text{Re}-\text{H})$ ionization is also affected by permethylation and shifts by 0.57 eV.

Similar effects of permethylation are observed for the metal bands of $\text{CpRe}(\text{NO})(\text{CO})\text{CH}_3$ and $\text{Cp}^*\text{Re}(\text{NO})(\text{CO})\text{CH}_3$. However, the ionizations labeled as Cp^* based for $\text{Cp}^*\text{Re}(\text{NO})(\text{CO})\text{CH}_3$ are destabilized by 1.30 eV from the Cp-based ionizations of $\text{CpRe}(\text{NO})(\text{CO})\text{CH}_3$, which is significantly more than for the hydrides. This shift is a hint that additional factors are influencing these ionization energies when a methyl ligand is present. Most striking is that the ionization assigned primarily to the $\sigma(\text{Re}-\text{C})$ bond ionization is *stabilized* slightly for $\text{Cp}^*\text{Re}(\text{NO})(\text{CO})\text{CH}_3$ as compared to $\text{CpRe}(\text{NO})(\text{CO})\text{CH}_3$. These shifts are evidence that simple assignment to

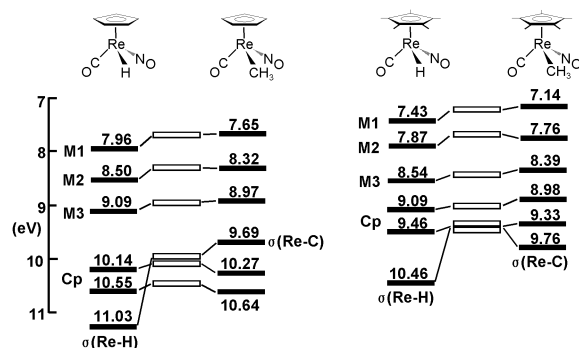


Figure 5. Trends in the ionization energies upon hydride to methyl ligand substitution. See the discussion of the projected shifts indicated by the open rectangles.

single fragment orbitals of Cp and $\sigma(\text{Re}-\text{C})$ is inadequate and that the Cp and $\sigma(\text{Re}-\text{C})$ ionizations are being affected by interactions that will be discussed in more detail in the following section.

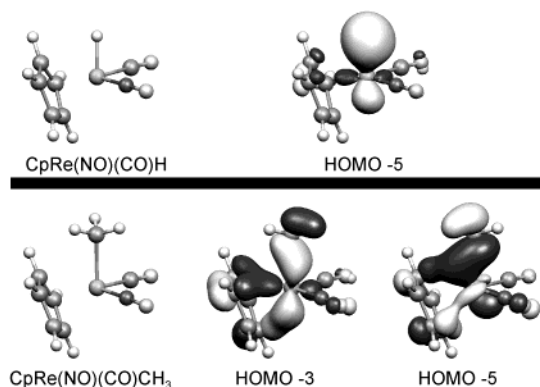
Effects of Methyl Substitution for Hydride at the Metal. From previous photoelectron studies of molecules of the general class CpML_2R , the Cp and M3 ionizations typically are affected primarily by charge potential effects of the R ligand and the Cp ionizations are observed to shift the same or slightly less than the M3 ionization with substitution of the R ligand.⁷⁶ A similar trend is found for the $\text{Cp}^*\text{Re}(\text{NO})(\text{CO})\text{R}$ molecules of this study, where the Cp^* -labeled ionizations shift in the same direction but slightly less than the M3 ionizations when a methyl ligand is substituted for the hydride ligand. For the $\text{CpRe}(\text{NO})(\text{CO})\text{R}$ molecules, however, the Cp-labeled ionizations do not track with the M3 ionization. Instead, the Cp-labeled ionizations are *stabilized* slightly on going from $\text{CpRe}(\text{NO})(\text{CO})\text{H}$ to $\text{CpRe}(\text{NO})(\text{CO})\text{CH}_3$, which again suggests that the corresponding Cp orbitals are involved in additional mixing.

The unusual trends in the Cp-labeled ionizations for the methyl molecules are explained by the interactions between the methyl σ donor orbital with the $[\text{CpRe}(\text{NO})(\text{CO})]^+$ fragment orbitals. Figure 5 summarizes the differences in ionization energies between the hydride and methyl molecules, with the connecting lines indicating the primary correlations. The open rectangles in Figure 5 show the expected ionization energies of $\text{CpRe}(\text{NO})(\text{CO})\text{CH}_3$ and $\text{Cp}^*\text{Re}(\text{NO})(\text{CO})\text{CH}_3$, as projected from the shifts of the corresponding ionizations of $\text{Mn}(\text{CO})_5\text{H}$ to $\text{Mn}(\text{CO})_5\text{CH}_3$ and of $\text{Re}(\text{CO})_5\text{H}$ to $\text{Re}(\text{CO})_5\text{CH}_3$.^{53,54} In the spectra of $\text{M}(\text{CO})_5\text{R}$ the d_{xz}/d_{yz} -based ionizations shift about 0.2 eV and the d_{xy} -based ionization shifts about 0.1 eV to lower energy when H is replaced by CH_3 . Most importantly, the $\text{M}-\text{CH}_3$ σ bond ionization is about 1.1 eV lower in ionization energy than the $\text{M}-\text{H}$ σ bond ionization. Using these shifts to project the ionization energies of $\text{CpRe}(\text{NO})(\text{CO})\text{CH}_3$ from those of $\text{CpRe}(\text{NO})(\text{CO})\text{H}$ places the $\text{Re}-\text{CH}_3$ σ bond just slightly less stable than the Cp levels. Although the overlap between the $\text{M}-\text{CH}_3$ σ bond orbital and the Cp orbitals (which also have some metal character) is small, the close energy proximity of the orbitals allows significant mixing. The effect of this mixing is shown in the comparison of the projected ionization energies with the observed ionization energies of $\text{CpRe}(\text{NO})(\text{CO})\text{CH}_3$ in Figure 5. The mixing causes

the Cp ionizations to be stabilized and the $\sigma(\text{Re}-\text{C})$ to be further destabilized.

In the spectrum of $\text{Cp}^*\text{Re}(\text{NO})(\text{CO})\text{CH}_3$, the order of the Cp^* and $\sigma(\text{Re}-\text{C})$ levels is reversed. Using the same $\text{M}(\text{CO})_5\text{R}$ shifts to project the ionization energies of $\text{Cp}^*\text{Re}(\text{NO})(\text{CO})\text{CH}_3$ from those of $\text{Cp}^*\text{Re}(\text{NO})(\text{CO})\text{H}$ places the $\text{Re}-\text{CH}_3$ σ bond ionization just slightly *more* stable than the Cp^* levels, because Cp^* ionizations are less stable than Cp ionizations. Further mixing between the $\sigma(\text{Re}-\text{C})$ and the Cp^* orbitals stabilizes the predominantly $\sigma(\text{Re}-\text{C})$ orbital and further destabilizes the predominantly Cp^* orbitals. The observed result is that the predominantly Cp^* ionization is at lower binding energy than the predominantly $\sigma(\text{Re}-\text{C})$ -based ionization. In fact, because of the near-degeneracy of the ionizations and the extensive mixing indicated by the shifts, not much significance should be placed on labeling one ionization $\sigma(\text{Re}-\text{C})$ and the other Cp^* .

The mixing and delocalization of the $\sigma(\text{Re}-\text{C})$ and Cp bonding framework, which is in contrast to the localized nature of the $\sigma(\text{Re}-\text{H})$ bond, is illustrated by the results of the density functional calculations on $\text{CpRe}(\text{NO})(\text{CO})\text{H}$ and $\text{CpRe}(\text{NO})(\text{CO})\text{CH}_3$ (surface value of ± 0.05):



The $\sigma(\text{Re}-\text{H})$ bond is essentially completely represented in the HOMO-5 orbital, while the $\sigma(\text{Re}-\text{C})$ bond is distributed among orbitals HOMO-3 and HOMO-5 that include the bonding of the Cp ring.

Metal-Based Ionizations. Thus far we have only addressed the σ bonding between the metal fragment and a hydride or methyl ligand. The ionizations also allow comparison of the π interactions of the ligands with the metal center. As described in Preliminary Theoretical Considerations, the M1 ionization corresponds to an orbital that has π symmetry with respect to the CO and R ligands, the M2 ionization corresponds to an orbital that has π symmetry with respect to the NO and R ligands, and the M3 ionization corresponds to an orbital that has π symmetry with respect to both the CO and NO ligands. For the hydride molecules the stabilization of M2 compared to M1 is then a measure of the greater π acceptor ability of NO compared to CO, while the difference in energy between the M2 and M3 ionizations is a measure of the ability of CO to stabilize a metal-based ionization by π back-bonding. Previous photoelectron studies of piano-stool molecules would project the energy splittings of M1, M2, and M3 to be about 0.7 eV. For $\text{CpRe}(\text{NO})(\text{CO})\text{H}$ the difference in energy between the M1 and M2 ionizations is actually 0.54 eV, while for $\text{Cp}^*\text{Re}(\text{NO})(\text{CO})\text{H}$ this value is 0.44 eV. A similar analysis of $\text{CpCr}(\text{CO})_2\text{NO}$ gives a value

of 0.79 eV.⁷⁸ These trends suggest that increasing electron richness at the metal center tends to level the differences between CO and NO π acceptor abilities to stabilize metal-based orbitals. For both CpRe(NO)(CO)H and $\text{Cp}^*\text{Re(NO)(CO)H}$ the difference in energy between M2 and M3 is 0.66 ± 0.02 eV. Previous studies on other piano-stool molecules give a CO π stabilization energy of 0.69 eV.^{56,76} The stabilization energy provided by a CO ligand has to this time not shown a significant dependence on the electron richness at the metal center.

The general agreement between the splittings of the metal-based ionizations in these molecules and those of previous studies indicates that spin-orbit coupling of the metal-based ionizations is not a major factor in the description of the electronic structure of CpRe(NO)-(L)R . This is also suggested by the reasonable agreement between the observed metal-based ionization energies and the DFT calculations of these energies, which do not include spin-orbit coupling in the calculations. Spin-orbit coupling is important to understanding the ionization energies of molecules that contain third-row transition metals when the metal-based ionizations are close in energy and localized on the metal center.^{54,55,79} The considerably different and large stabilizations provided by the nitrosyl and carbonyl ligands is one factor that minimizes the effects of spin-orbit coupling. Another likely factor is the extent of delocalization of the metal-based orbitals.

The changes in relative intensities of the metal-based ionizations between the He I and He II spectra show that these ionizations are not similarly delocalized from the metal center. On the basis of the relative cross-sections mentioned earlier, those ionizations with the most oxygen character will maintain their intensity best from the He I to the He II spectra. The oxygen character in the metal-based ionizations is a consequence of the π back-bonding into the carbonyl and nitrosyl ligands. The M3 ionization, which involves back-bonding into both CO and NO, maintains its intensity better than the M2 ionization, which involves back-bonding only to the NO ligand, and the M2 ionization maintains its intensity better than the M1 ionization, which has weaker back-bonding to the CO ligand. These intensity changes again indicate little spin-orbit mixing of the metal-based ionizations, which would tend to level these effects. The different extents of delocalization of the metal-based orbitals by the different ligands are important to later discussion.

Methyl π Interaction. One fundamental question addresses the ability of a methyl ligand to act as a π donor ligand. As shown earlier, the methyl ligand includes an occupied e set of C-H bonding orbitals that are able to act as π donors with respect to the metal.⁷⁰⁻⁷² Just as the shifts of the metal-based ionizations are sensitive to the π stabilizations provided by back-bonding ligands, they are also sensitive to the filled-filled interactions with π donor ligands. In CpRe(NO)-(CO)R replacing the hydride ligand with a methyl causes the M1, M2, and M3 metal-based ionizations to be destabilized by 0.31, 0.18, and 0.12 eV, respectively. The general destabilization of the ionizations reflects

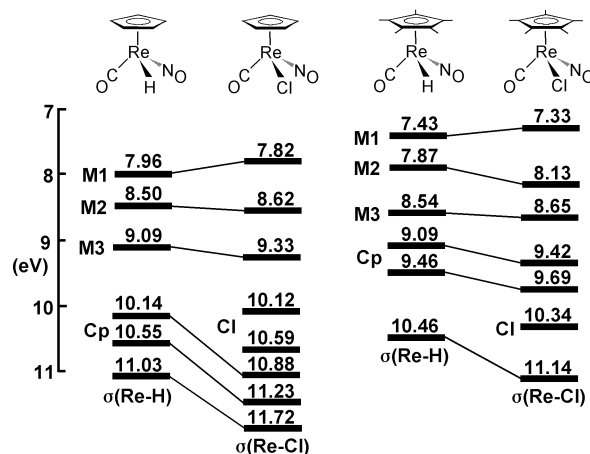
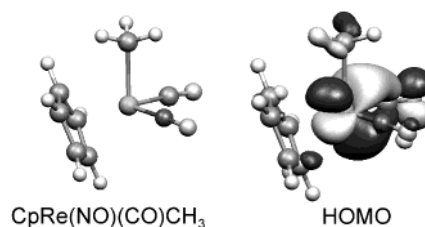


Figure 6. Trends in the ionization energies upon hydride to chloride ligand substitution.

the better overall donor ability of the methyl ligand. Additionally, the much larger shift of the M1 ionization suggests that the corresponding orbital is being destabilized by an additional filled-filled interaction with the occupied methyl e set orbitals. The same interaction can occur with M2; however, the M2 ionization shifts less than M1 (but still more than M3). The very efficient π^* acceptor orbitals of NO cause a greater delocalization of the $\text{M2}_{\text{NO,R}}$ orbital onto the NO ligand and reduces the overlap of this orbital with the methyl π orbitals compared to M1. In $\text{Cp}^*\text{Re(NO)(CO)R}$ and $\text{CpRe(NO)-(PPh}_3\text{)R}$ the same trends are observed when the hydride is replaced with a methyl ligand. The M1 is destabilized to a much greater degree than the other metal bands.

The π -type interaction between the metal and the CH_3 ligand is also evident in the computational results. HOMO and HOMO-1 are destabilized more than HOMO-2 for CpRe(NO)(CO)CH_3 as compared to CpRe(NO)-(CO)H , and there is orbital contribution from the CH_3 ligand to HOMO and HOMO-1. The calculations do not show the larger destabilization of the HOMO as compared to HOMO-1 that would have been expected from the experimental results. The filled-filled π -type interaction between the metal and the CH_3 ligand indicated by these ionization energy shifts is illustrated by the surface contour of the HOMO of CpRe(NO)(CO)CH_3 (surface value of ± 0.05):



The orbital is predominantly metal d_{yz} with substantial back-bonding to the CO π^* orbital and includes a contribution from the methyl ligand that is π antibonding with respect to the metal density.

Previous studies on CpRe(NO)(CO)X and $\text{Cp}^*\text{Re(NO)-(CO)X}$ ($X = \text{Cl, Br, I}$) suggested that the halide ligands also act as good π donors in these systems.⁵² Comparison of the ionizations of the hydride and chloride molecules, shown in Figure 6, confirms this. There is a general

(78) Lichtenberger, D. L.; Hubbard, J. L. *Inorg. Chem.* **1980**, *19*, 1388-1390.

(79) Hubbard, J. L.; Lichtenberger, D. L. *J. Am. Chem. Soc.* **1982**, *104*, 2132-2138.

stabilization of the ionizations when the hydride ligand is substituted by chloride, which reflects the electronegativity and subsequent poorer σ donor ability of the chloride ligand. Specifically, the M2 and M3 ionizations are stabilized, but the M1 band is *destabilized*. The Cl $p\pi$ lone pair orbital interacts with the M1_{CO,R} orbital in a filled-filled interaction that stabilizes the Cl $p\pi$ orbital and destabilizes the $d\pi$ orbital. The metal-chloride π interaction is about twice that of the metal-methyl π interaction. The chlorine p_y lone pair orbital also has the proper symmetry to interact with the M2_{NO,R} orbital; however, the lack of destabilization of the M2 ionization again shows that the NO ligand is able to diminish the magnitude of the overlap interaction. The only halide which shows a stronger π interaction with M2 over M1 is iodide, for which extremely good energy matching between the iodide $p\pi$ and M2 appears to be sufficient to overtake the more efficient π overlap with M1.

Comparison of CpRe(NO)(CO)R and CpRe(NO)-(PPh₃)R. The metal ionizations in CpRe(NO)(PPh₃)R can be used to show the effect of substituting a phosphine for a carbonyl. The electronic effects of phosphine substitution for CO on the metal ionizations in other systems have been documented.^{80–83} A phosphine ligand substituted in place of a carbonyl places extra negative charge potential at the metal center, which destabilizes all the ionizations. When the spectrum of CpRe(NO)-(PPh₃)H is compared to that of CpRe(NO)(CO)H, the three metal-based ionizations have all been destabilized by over 1 eV. These shifts are similar to those observed for the metal ionizations of CpMn(CO)₂(PPh₃) as compared to CpMn(CO)₃ and of Mo(CO)₅(PPh₃) as compared to Mo(CO)₆.^{81,84} The previous studies also showed that the PPh₃ ligand stabilized metal-based ionizations through π back-bonding by about 0.4 eV, in comparison to the 0.7 eV stabilization provided by CO. The predicted difference between the M1 and M2 ionization energies (using 1.4 eV for the stabilization of M2 by NO and 0.4 eV for the stabilization of M1 by PPh₃) is about 1 eV. The observed difference between M1 and M2 is found to be 0.92 eV for CpRe(NO)(PPh₃)H and 1.04 eV for CpRe(NO)(PPh₃)CH₃. The difference between the M2 and M3 ionizations, which is approximately the extra stabilization provided by PPh₃, is 0.42 eV for CpRe(NO)-(PPh₃)H and 0.48 eV for CpRe(NO)(PPh₃)CH₃.

In CpRe(NO)(PPh₃)R replacing the hydride ligand with a methyl causes the M1, M2, and M3 ionizations to be destabilized by 0.22, 0.10, and 0.04 eV, respectively. Again, M1 is destabilized more than M2, which is destabilized more than M3. These shifts are smaller than those observed for CpRe(NO)(CO)R, indicating that as the electron density at the metal center is increased by replacement of CO by PPh₃ and the orbital energies are destabilized, the π interaction from the methyl ligand is decreased.

Electronic Control of the Stereoselective Binding of R Ligands. As shown by a number of observations from the photoelectron spectra discussed to this point, the methyl ligand has a stronger π interaction with M1 than it does with the other $d\pi$ orbital, M2. The preferential π interaction of R ligands with M1 instead of M2 has also been ascertained from structural studies of CpRe(NO)(L)R, where L is PPh₃ and R is a single-faced π -acceptor ligand such as η^2 -aldehyde,⁵¹ carbene, or vinylidene.^{85,86} For these molecules, the more efficient π interaction translates into a preferential binding geometry that maximizes π overlap between M1 and the sole R ligand-based π acceptor orbital and results in only one set of diastereomers being formed for these chiral complexes.

The preferential binding geometry of [CpRe(NO)(L)]⁺ with π acceptor ligands has been attributed previously to the ligand π acceptor orbital having a better energy match with the M1 orbital than with the M2 orbital.^{51,87} The photoelectron spectra of the hydride molecules reported here give the first experimental information on the relative energies of the M1 and M2 $d\pi$ orbitals, since the energy splitting of the $d\pi$ orbitals of the hydride molecules and [CpRe(NO)(L)]⁺ should be the same. As described earlier, the energy difference between these two orbitals is directly related to the difference in π acceptor abilities of the NO and L ligands, such that the energy splitting between M1 and M2 is about 0.5 eV when L is CO but is increased to about 1.0 eV when L is PPh₃.

While the destabilization of M1 as compared to M2 explains the greater interactions of M1 with π acceptor ligands, the methyl ligand, which acts as a π donor, also interacts to a greater extent with M1. The preferential interaction of ligand π -donor orbitals with M1 over M2 is dominated by increased overlap, not energy matching. In the case of π donor ligands such as methyl, phosphine substitution for carbonyl creates competing influences of poorer orbital energy match but better orbital overlap. The photoelectron spectra of the metal-methyl complexes give a measure of which effect is most important for each metal-based orbital. The overlap effect is found to be most important for the M1 ionizations when methyl replaces hydride in these molecules.

Conclusions

The experimental results presented here show that several orbital interactions are important in an overall description of the metal-methyl bond in these systems, while the metal-hydride bond remains essentially localized even in these low-symmetry molecules. The extent of the metal-methyl interactions and the resultant delocalization is strongly dependent on the energy proximity of the orbitals. First, there is mixing between the Cp-Re and Re-CH₃ σ bonding orbitals that has

(80) Bursten, B. E.; Darensbourg, D. J.; Kellogg, G. E.; Lichtenberger, D. L. *Inorg. Chem.* **1984**, *23*, 4361–4365.

(81) Bancroft, G. M.; Dignard-Bailey, L.; Puddephatt, R. J. *Inorg. Chem.* **1986**, *25*, 3675–3680.

(82) Hu, Y.-F.; Bancroft, G. M.; Davis, H. B.; Male, J. I.; Pomeroy, R. K.; Tse, J. S.; Tan, K. H. *Organometallics* **1996**, *15*, 4493–4500.

(83) We, J.; Bancroft, G. M.; Puddephatt, R. J.; Hu, Y. F.; Li, X.; Tan, K. H. *Inorg. Chem.* **1999**, *38*, 4688–4695.

(84) Rempe, M. E. Ph.D. Dissertation, The University of Arizona, 1994.

(85) Senn, D. R.; Wong, A.; Patton, A. T.; Marsi, M.; Strouse, C. E.; Gladysz, J. A. *J. Am. Chem. Soc.* **1988**, *110*, 6096–6109.

(86) Brady, M.; Weng, W.; Zhou, Y.; Seyler, J. W.; Amoroso, A. J.; Arif, A. M.; Bohme, M.; Frenking, G.; Gladysz, J. A. *J. Am. Chem. Soc.* **1997**, *119*, 775–788.

(87) Kiel, W. A.; Lin, G.-Y.; Constable, A. G.; McCormick, B. F.; Strouse, C. E.; Eisenstein, E.; Gladysz, J. A. *J. Am. Chem. Soc.* **1982**, *104*, 4865–4878.

(88) Le Bras, J.; Jiao, H.; Meyer, W. E.; Hampel, F.; Gladysz, J. A. *J. Organomet. Chem.* **2000**, *616*, 54–66.

observable effects on the ionizations of the methyl molecules. Second, the methyl ligand is shown to be acting as a weak π donor ligand. The photoelectron spectra provide quantitative measure of the π -donor ability of CH_3 to destabilize the metal-based levels.

This study furthermore provides a paradigm for future analyses of the comparative electronic structures of metal hydride and alkyl complexes. The exact differences are a sensitive function of many factors, among which are the metal, ligand set, and orbital occupancy. Importantly, even small differences can be expected to have a profound effect on many phenomena. One example would be the relative thermodynamics of β -hydride versus β -alkyl elimination from coordinatively unsaturated metal alkyl complexes—two competing steps that determine key properties of many alkene polymers. The experimental and theoretical elucidations

of such subtle underlying electronic factors, and their correlation to thermodynamic, structural, and reactivity characteristics, constitute one of the most important future challenges for chemistry.

Acknowledgment. D.L.L. thanks the U.S. Department of Energy and the National Science Foundation (Grant No. 0078457) for support. J.A.G. thanks the U.S. National Science Foundation and the Deutsche Forschungsgemeinschaft (Grant No. SFB 583) for support.

Supporting Information Available: Tables of calculated total electronic energies and coordinates for optimized geometries. This material is available free of charge via the Internet at <http://pubs.acs.org>.

OM020793T